Optimization of Isomerization Activity and Aromatization Activity in Catalytic Naphtha Reforming over Tri-Metallic Modified Catalyst using Design of Experiment Based on Central Composite Design and Response Surface Methodology

Fawzi M. Elfghi[1,*], N.A.S. Amin[2] and Mohammed M. Elgarni[3]

[1]*Malaysia-Japan International Institute of Technology (MJIIT), Department of Environment and Green Technology (EGT), Universiti Teknologi Malaysia (UTM), 54100 UTM, Jalan Semarak, Kuala Lumpur, Malaysia*

[2]*Chemical Reaction Engineering Group (CREG), Faculty of Chemical Engineering, Universiti Teknologi Malaysia, 81310 UTM, Skudai, Johor, Malaysia*

[3]*HTC Purenergy Inc. #150-10 Research Drive, Regina, Saskatchewan, Canada*

Abstract: In this work, the estimation capacity of the response surface methodology (RSM), in the catalytic naphtha reforming to enhance the octane number of reformats via isomerization reaction pathway and minimize the aromatization activity over tri-metallic modified Pt-Re/Al_2O_3 catalyst were investigated by applying Design of experiment (DOE). The parent bimetallic catalysts were modified using a relatively inactive metal (Sn) by means of employing non-conventional method of anchoring technique called controlled surface reaction (CSR) method in order to favor the intimate contact of Sn with the active phase to suppress the metallic character of Pt metal. The correlations between RON, aromatization and isomerization activities with three reaction variables namely temperature (480-510^oC), pressure (10-30 bar) and space velocity LHSV (1.2-1.8 h^{-1}) were presented as empirical mathematical models via reforming of a complex mixture (80^oC -185^oC). Numerical results indicated that the minimum aromatization activity was 20% when reaction temperature was 460^oC and pressure of 35 bar. Results also show that maximum isomerization activity of 58% was achieved when pressure is 30 bar and space velocity is 1.8 h. it has been found that optimum value of RON = 89 was attained at 449.9^oC, 32 bar and 1.7 h^{-1}. However, high operating pressure and low reaction temperature significantly decrease the aromatization activity coupled with substantial decrease in RON which can be enhanced by producing high yield of isomers.

Keywords: Catalytic naphtha reforming, Central composite design, Design of experiment, Response surface methodology, Tri-metallic catalyst.

INTRODUCTION

Gasoline fuel considered as the most important product at oil refineries. Gasoline pool is a blend of various streams produced from different catalytic units such as catalytic naphtha reforming, fluid catalytic cracking (FCC), alkylation and hydrocracking, includes additives such as MTBE to enhance the octane number of the finished gasoline. Nowadays, attention of refiners have shifted to other sources of octane boosters in the reformulated gasoline pools [1] due to environmental guidelines such as elimination of MTBE as additive [2, 3] and limitation in the content of total aromatics particularly benzene [4, 5]. Branched chain alkanes have higher octane number than straight alkanes; the use of such compounds is a suitable route for providing an alternative in obtaining fuel with the required characteristics since they improve the octane number of the gasoline pool for cleaner fuels [6, 7]. However, the selectivity towards branched hydrocarbons is limited over the currently used Pt-Re catalyst due to the competitive reactions that occur simultaneously and subsequently. In the catalytic reforming over bi-functional Pt-Re/Al_2O_3-Cl catalyst, the liquid yield (C_5^+), yield of aromatics, iso-paraffin/aromatics ratio and side reactions can be altered by the optimization of independent variables, amending of injected chlorine or the addition of different promoters to the catalyst such as Ge, Sn, Ir, etc. In this regard, several publications have been reported pertaining the effects and optimization of operating conditions in the reforming of model compounds and real feedstock's using one-variable-at-a-time-approach (OVAT) [8- 10]. However, OVAT has some major imperfections because the experimental space is not explored very well and the solution may be missed if there are interactions among the variables. Moreover, it is expensive and time consuming, especially when a huge number of parameters are to be examined. To bypass this difficulty to estimate and understand the interactions

*Address correspondence to this author at the Malaysia - Japan International Institute of Technology (MJIIT), UTM Kuala Lumpur, Jalan Semarak, 54100 Kuala Lumpur; Tel: 60 18-968 0307; Fax: +603 - 2203 1266;
E-mail: felfghi@gmail.com/fawziamin@ic.utm.my

E-ISSN: 2408-9834/15

between different variables, recently, DOE coupled with response surface methodology (RSM) approach based on performing of CCD experiments become very well documented and widely employed. It is currently used for optimization studies in several biotechnological and industrial processes. RSM is a set of a group of empirical techniques devoted to estimating interaction and quadratic effects. It also gives an idea of the local shape of investigating response surface. RSM is practically used to reveal the best value of the response, find out improved or optimal process settings, and troubleshoot process problems and weak points [11-14]. However, the evaluation of pilot plant performance for naphtha reforming catalysts is complicated because of the variety of successive reactions taking place subsequently. Hence, the development and adaptation of detailed experimental procedures are extremely important in order to attain reliable data [15].

Literature has shown that parameters such as temperature, pressure and space velocity affected the catalytic performance of naphtha reforming process. Therefore, the objective of this work was to investigate the catalytic performance of modified tri-metallic Pt-Re-Sn catalyst using a relatively inactive metal (Sn) by means of employing non-conventional method of anchoring technique to suppress the high metal character of Pt in order to maintaining high RON via isomerization reaction pathway and minimize the selectivity towards aromatics hydrocarbons. The Controlled surface reaction method was chosen to favor the intimate contact of Sn with the active phase of Pt–Re catalyst. Furthermore, the effects of process parameters and their interactions on the catalytic performance were studied simultaneously on the responses using design of experiments (DOE). We report the use of a statistical approach called Central Composite Rotatable Design (CCRD) falling under Response Surface Methodology (RSM) to predict the optimum values of process parameters and their interactions for single and multi-response optimization; maximum *RON* via isomerization pathway and minimize the selectivity towards aromatics hydrocarbons.

EXPERIMENTAL AND METHODS

Catalysts Preparation

An industrial applied catalyst was used in this study. The size of the catalyst pellets were in the range of 1.5 to 2.0mm. The catalysts composed of dual function components that consisted of the catalytic active species Pt (0.17 wt %) for hydrogenation and dehydrogenation reactions and Re (0.35 wt %) as a promoter, supported on chlorinated Al_2O_3-Cl (Cl = 1.34 wt. %). The chlorinated compound also worked as an acid component, catalyzing both isomerization and cyclization reactions. The tri-metallic Pt-Re-Sn (0.32) catalyst was prepared using controlled surface reaction method via a circulation glass reactor making use of pre-absorbed hydrogen on Pt and organometallic precursor $Sn(C_2H_5)_4$. The bimetallic catalysts were first purged at 150^oC in nitrogen atmosphere for 1 hr. and then reduced at 500 ^oC for 2 h in hydrogen (60 cm^3 min^{-1}), cooled down to the modification temperature while maintaining the hydrogen flow. The catalyst bed was wetted with the solvent (free sulf1ur naphtha) and saturated with hydrogen for additional 30 minutes. Then an appropriate calculated concentration of Sn $(C_2H_5)_4$ solutions were intervals injected via the septum located at the top of the reactor and circulated using micro pump of 150 ml/min flow and temperature of 50^oC. After 1 h of contact time under constant hydrogen flow (300 cm^3 min^{-1}), the solution was drained after switching off the atmosphere in the reactor to argon. Next, the washing procedure started at 50^oC to remove un-reacted precursor anchored on the support. Then the catalyst bed was dried under vacuum for 2h then purged at 50 ^oC under argon overnight. Finally, the catalyst undergoes decomposition step of (PSC) Primary Surface Complex under hydrogen atmosphere using temperature programmed reduction technique (TPR) of 25-350^oC. The metal content of base and modified catalysts determined by Atomic Absorption Spectroscopy (AAS) and Inductivity Coupled Plasma spectroscopy (ICP) techniques using (*VISTA-PRO CCD SIMULTANEOUS ICP-OES*) device were comparable. Good agreement was found between nominal and evaluated tin content.

CATALYSTS CHARACTERIZATION

A LEO-1430 VP microscope instrument was used in which the EDX system IXRF was installed. The microscope has a magnification power up to 300,000 times and was operated at 2.0-30 kV with two guns; tungsten gun filament and L_aB_6 gun filament equipped with back scattered detector. The point to point resolution of the instrument was 2.5 A^o at high vacuum and 5 A^o at low vacuum. The energy resolution of the EDX system was 133 eV at 5.9 keV. The pretreatment of the catalyst sample was performed by coating with gold powder and placed in the electron optics column then evacuated to $2*10^{-6}$ torr. The highest magnification used was 200,000 times with a resolution

of 10 nm at a working voltage of 15 kV.

The parent and modified samples were crushed and sieved. The particles with a mesh size of 120 to 200 were used for XRD analysis. X-ray diffraction experiments were performed in an X-ray powder diffractometer (PW 1800, Automatic powder Diffractometer system, Philips Analytical X-Ray). The ground samples were analyzed with Cu Kα radiation. The samples were scanned in the range of 2θ = 10–80◦ at a scanning speed of 2◦/min.

Nitrogen physisorption experiments for BET surface area measurements were determined by nitrogen adsorption/desorption at 77 K, data acquired on a *Micromeritics ASAP 2010* apparatus. The samples were de-gassed overnight at 350 ^{o}C under vacuum of $5x10^{-3}$ Torr for 15 h to eliminate moisture of adsorbed water and some of impurities. The total surface areas of the parent and modified samples were calculated using the BET equation.

CATALYTIC ACTIVITY TEST

Catalytic reforming tests were performed using a high-pressure catatest unit from GEOMECHANIQUE, FRANCE. The unit consisted of a fixed-bed down-flow laboratory isothermal reactor in once-through mode designed to be operated up to 150 bar and 700^{o}C. The reactor has an internal diameter of 19 mm and volume of 150ml with five jackets heating zones. The loaded catalyst of 55 g (70 ml) was placed between two layers of inert particles of silicon carbide (carbines). Prior to the activity test, the catatest unit underwent leakage test. The unit was pressurized under the flow of nitrogen up to 90 bars. After the attainment of 90 bar, this pressure was maintained for 120 min. Throughout this period, leakage was not detected. After confirming that there was no leak (less than 0.1 MPa/h), the unit was depressurized and the operating conditions were adjusted to the required activity test conditions for the design of experiments matrix runs.

FEED AND PRODUCT ANALYSIS

The feed consisted of hydro-treated virgin naphtha having a boiling range of 80-185 ^{o}C. The feed and product distribution of liquid hydrocarbons was determined using Near Infra Red (NIR) Portable Petro-Spec Gasoline Fuel Analyzer. From the analysis of reformate composition the following parameters were obtained: RON, i-paraffins, and aromatics. Table **1** tabulates the composition and Research Octane Number RON of the feed. Reformate samples of liquid products were collected for each condition after 45 min equilibrium time every hour for 240 min time- on-stream (TOS).

DESIGN OF EXPERIMENTS (DOE)

A complete description of the process behavior requires a quadratic or higher order polynomial model. Hence, the full quadratic models were established by using the method of least squares, which includes all interaction terms to calculate the predicted response. The quadratic model is usually sufficient for industrial applications. For n factors the full quadratic model is shown in Eq. (1)

$$Y = b_o + \sum biXi + \sum b_{ij}X_iX_j \ (I,j = 1,2,3,\ldots..,k) \quad (1)$$

Where *Y* is the predicted response or dependent variable, X_i and X_j are the independent variables, and *bi* and *bj* are constants. In this case, the number of independent factors is three and therefore, k = 3: Eq. (1) becomes Eq. (2):

$$Y_u=\beta_o+\beta_1X_1+ \beta_2 X_2+ \beta_3 X_{3+} \beta_{12} X_1X_2+ \beta_{13}X_1X_3+ \beta_{23}X_2X_3+ \beta_{11}X_1^2+\beta_{22}X^2_2+\beta_{33}X_3^2 \quad (2)$$

With *Y* being the predicted response, X_1, X_2 and X_3 are the coded forms of the input variables for reaction temperature, operating pressure and space velocity, respectively. The term β_o is the intercept term; β_1, β_2 and β_3 the linear terms; β_{11}, β_{22} and β_{33} are the squared terms; β_{12} β_{13} β_{23} are the interaction terms between the three variables. The selection of these variables with their defined experimental ranges were carefully chosen based on previous screening tests prior to optimization and are often used in literatures. The lowest and the highest levels of variables coded as -1

Table 1: Total Hydrocarbons by Group Type and RON of Virgin Naphtha Determined by NIR Gasoline Analyzer

∑ Aro. wt.%	i-parf wt.%	Naph. wt.%	Olf. wt.%	Paff. wt.%	C_6A wt.%	C_7A wt.%	C_8A wt.%	RON
3.4	27.2	44.5	1.1	33.7	0.0	0.2	1.6	64.3

Abbreviations: ∑ Aro: total aromatics; i-parf: iso-parffins; Olf: olefins; Parff. : Paraffins; Naph. : naphthenes; $C_{6,7,8}A$ aromatics; *RON*: research octane number

Table 2: Independent Variables and their Coded and Actual Values

Independent Variable	Symbol	Coded Levels				
		-α	-1	0.00	+1	+α
Operating temperature (◦C)	X_1	468	480	495	510	521
Operating pressure (bar)	X_2	2	10	20	30	37
L.H. Space velocity (h^{-1})	X_3	0.9	1.2	1.5	1.8	2.0

Where: −/+α, star point value; −1, low value; +1, high value; 0, center value.

and +1, respectively are given in Table **2** including axial star points of (- *α* and + *α*), where *α* is the distance of the axial points from centre and makes the design rotatable.

In this study *α* value was calculated using Eq. (3) and was fixed at 1.68 (Rotatable).

$$\alpha = (F)^{1/4} \quad (3)$$

Where *F* is the number of points in the cube section of the design ($F = 2^k$, k is the number of factors). Since we have three factors, the *F* number is equal to 2^3 (= 8) points, and *α* = 1.68. Therefore, the total number of experiment combinations should be conducted based on the same concept of CCRD by applying Eq. (4)

$$2^k + 2k + n_o \quad (4)$$

Where k is the number of independent variables and n_o is the number of experiments repeated at the centre point. In this case, $n_o = 2$ and k = 3 give the total number of runs needed as 16. A matrix of 16 experiments with three factors was generated using the software package, '*STATISTICA* version 6 (*StatSoft Inc., Tulsa, USA*). The two centre points were used to determine the experimental error and reproducibility of the data. Table **3** tabulates the complete design matrix of the experiments performed together with the results

Table 3: Central Composite Design Matrix and Experimental Results

Standard Run		X_1		X_2		X_3		RON	Aromatization Activity	Isomerization Activity
		Reaction Temperature (°C)	level	Operating Pressure(bar)	level	LHSV(h^{-1})	level			
1	R	480	-1	10	-1	1.2	-1	98.6	60.50	38.20
2	R	480	-1	10	-1	1.8	1	98.06	59.51	37.78
3	R	480	-1	30	1	1.2	-1	92.30	43.70	55.23
4	R	480	-1	30	1	1.8	1	91.40	40.45	58.00
5	R	510	1	10	-1	1.2	-1	105.1	77.50	19.60
6	R	510	1	10	-1	1.8	1	100.53	65.13	32.73
7	R	510	1	30	1	1.2	-1	98.90	66.2	23.30
8	R	510	1	30	1	1.8	1	101.0	66.73	32.10
9	C1	495	0	20	0	1.5	0	95.70	52.5	47.30
10	R	469.77	-α	20	0	1.5	0	91.50	40.88	57.00
11	R	520.22	+α	20	0	1.5	0	103.7	55.00	42.20
12	R	495	0	3.18	-α	1.5	0	101.5	66.25	25.33
13	R	495	0	36.81	+α	1.5	0	98.90	48.30	50.30
14	R	495	0	20	0	0.97	-α	100.50	67.60	36.40
15	R	495	0	20	0	2.02	+α	90.80	41.50	56.70
16	C2	495	0	20	0	1.5	0	95.70	52.50	47.30

Where: R = Rotatable design points, C = centre points, S = star axial points. -1=low value, +1=high value,+/- α= star point value.

obtained. The responses were used to develop an empirical model for RON (Y_{RON}), aromatization activity (Y_{Aro}) and isomerization activity (I_{somers}).

After executing the experimental design, interpretations and analyses of the experimental data were determined by employing Analysis of Variance (ANOVA) at 5% level of significance using Fisher *F-test*. The *F-test* is a simple arithmetical method that sorts the components of variation in a given set of data and provides test for significance.

RESULTS AND DISCUSSION

Characterization

The effect of introduced tin to the catalyst (Pt-Re-(Sn-0.32)), on the SEM images was almost negligible to be noticed and not very remarkable since the concentration of introduced tin was too small and present as a highly dispersed oxide (SnO). Figures **1** and **2** show images of parent and modified catalyst with a resolution at around 7.73 *KX*. They appear bright spots areas most likely corresponding to platinum particles on the porous of Alumina.

In the EDX patterns, the majority of metal particles detected were platinum, Rhenium, Ferric, and Sn. The Al, O and Cl peaks in all spectrums was attributed to the chlorinated alumina support. However, Fe peaks revealed to some impurities generally present in the commercial catalyst. Some peaks representing gold (Au) usually indicate radiation from the metal coating and the specimen plug so should be ignored. A considerable overlapping of *X-ray* intensity on the *M* axis between Pt and Au as well as Re were due to the closeness of Pt (2.05 keV) and Au (1.89 keV) in the periodic table. The *EDX* quantitative analysis confirmed the presence of tin, suggesting that part of it reduced and alloyed with platinum during the modification step under hydrogen atmosphere resulting in reduce the accessibility of Pt peaks in the modified samples.

The XRD patterns shown in Figures **3** and **4** show only three peaks located at 37.32, 46.12, and

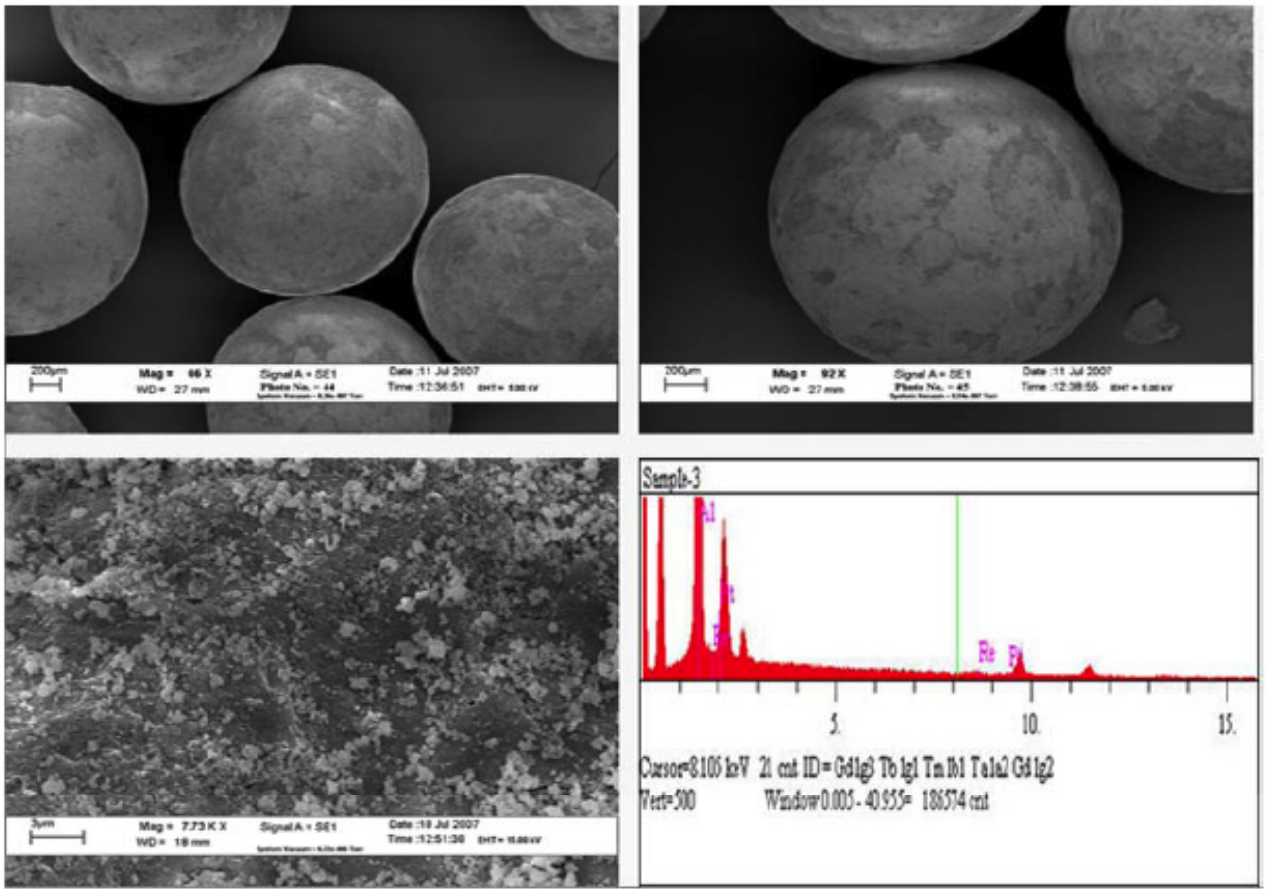

Figure 1: SEM images at low and high resolutions coupled with EDX patterns of Pt-Re/Al2O3 parent catalyst.

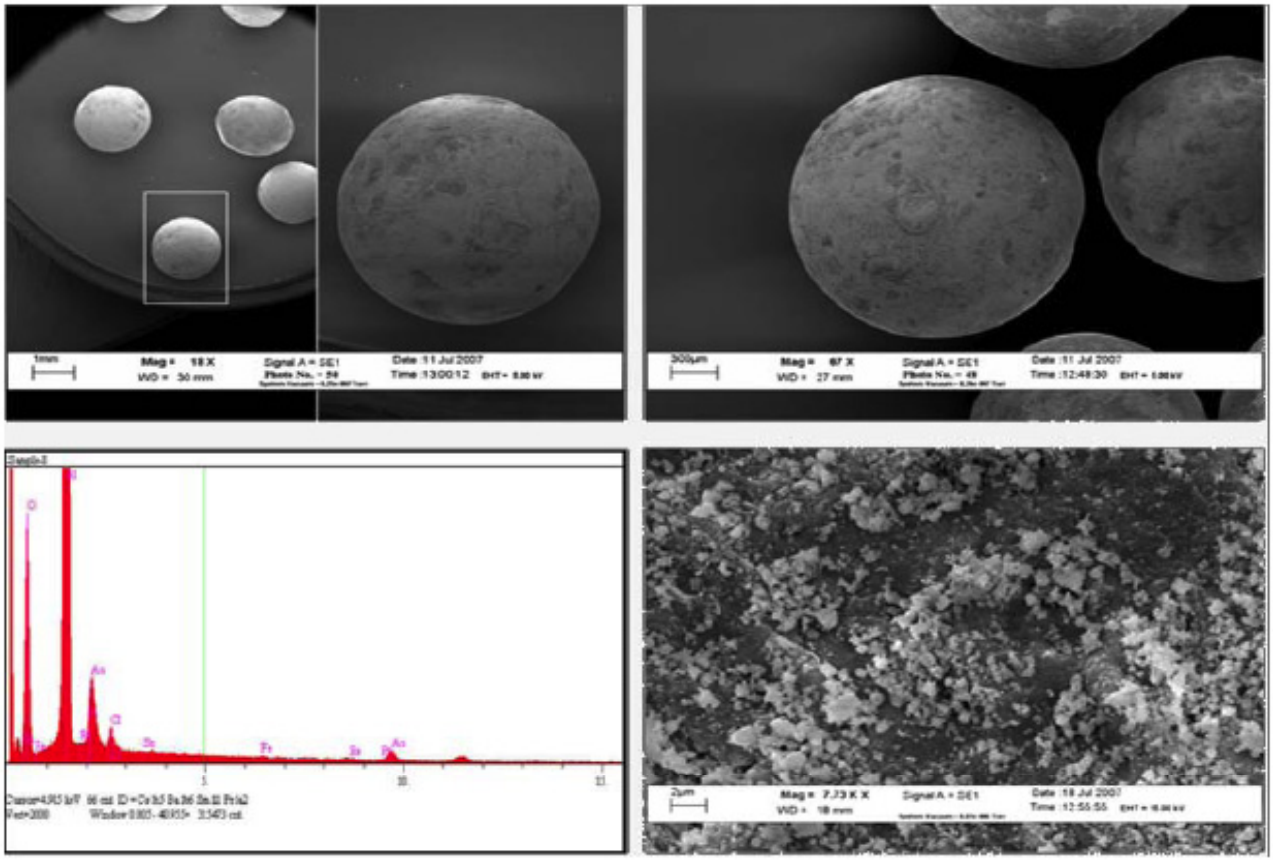

Figure 2: SEM images at high and low resolutions coupled with EDX pattern of Pt-Re-Sn (0.32)/AlO3 modified catalyst.

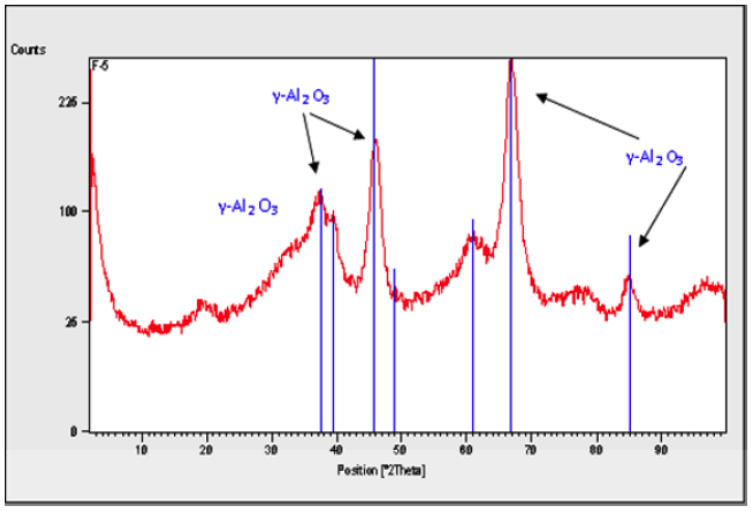

Figure 3: XRD patterns of Pt-Re/Al2O3 catalysts.

66.92, respectively of *2θ* attributed to *γ*- alumina and demonstrate its semi crystanallity. Based on previous studies on metal supported catalysts characterized by *XRD*, the presences of metal that can be detected in the catalyst depend on the amount of metal loaded and calcination temperatures. Since the concentrations of Pt, Re and Sn are too small and they contributed in the catalyst system as amorphous materials, hence no peaks of these metals were detected. Furcht *et al*. [16] reported that when the support is alumina for Pt reforming catalyst, the Pt 4f peak usually cannot be detected because of the large Al *2p* peak of the

support, while the smaller Pt *4d* signal was below the detection limit. Indeed, this result demonstrated that the structure of the parent catalyst network didn't collapse as a result of anchoring with Sn species.

Table **4** shows the following: (i) Parent catalyst of 0.0.wt% of Sn shows high BET surface area value, (ii) loading Pt-Re with Sn (0.32%) brought about a considerable decrease in the total surface area values. It was noticed that the pore volume and average pore diameter were moderately affected upon the introduction of Sn to the parent catalyst. This can be attributed to the miss control of the introduced metal throughout the anchoring step of Sn_2 $(C_2H_5)_4$ during the modification procedure, since some of the un-controlled species of tin deposited on the support as Al-O-M. It can reveal that small amount of adsorbed Sn atoms were mostly dispersed on the outer layer of the support.

RON Model (Single-Response Optimization)

The optimal values of the three manipulated variables in the Pt-Re-Sn catalyst such that maximum RON is achieved with a maximum isomerization activity and minimum aromatization activity are presented in this section. The experiments were performed according to the designed matrix in Table **3**. The coefficients of the models developed in Eq. (2) were estimated using multiple regression analysis technique. The quadratic mathematical model of RON (Y_{RON}) is represented in Eq. (5).

$$Y_{RON} = 805.3954 - 2.9024x_1 - 4.1514x_2 + 1.8125x_3 + 0.0060x_1x_2 - 0.0286x_1x_3 + 0.2629x_2x_3 + 0.0031x_1^2 + 0.0153x_2^2 + 0.7218x_3^2 \quad (5)$$

The fitness of the models developed was arbitrated from the determination of the correlation coefficient value, R^2. A practical rule of thumb for evaluating the determinant coefficient, R^2 is that it should be higher or equal 0.75 [17], which explain the total deviation of the observed values of activity about its mean [18–21]. The closer the R^2 value to unity, the better the model will be, as it will give predicted values closer to the actual values for the response as depicted in Figure **5**. In this case, the value of R^2 = 0.885 indicates that there is a good agreement between the observed and predicted values of RON from the fitted model.

The adequacy of the RON model was checked by ANOVA. Generally, the Fisher test value is a measurement of variance of data about the mean based on the ratio of mean square of group variance due to error [22]. The *F*-computed value should be higher than the tabulated value for the model to be considered as good predictor model. In this study, the calculated Fisher test values for the RON model shown

Table 4: BET Surface Area Results of Reference and Modified Catalysts

Catalyst	BET (m^2/g)	Pore volume (cm^3/g)	Pore size (A°)
Pt-Re/Al_2O_3	245.7	0.467	114.3
Pt-Re-Sn/Al_2O_3	185.5	0.5279	113.82

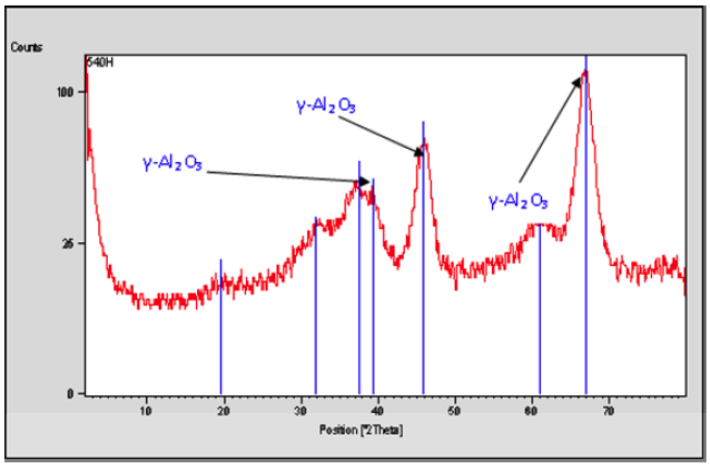

Figure 4: XRD patterns of Pt-Re-Sn (0.32) /Al2O3 modified catalyst

in Table **5**, are greater than the tabulated *F*-value ($F_{6, 9, 0.05}$ = 3.37) at α = 0.05 in statistic tables [23]. By that virtue, the null hypothesis (H_o) was rejected and it can be deduced that the model has a good prediction of the responses. The calculated *F*-value corresponding to RON model is 5.147 greater than the tabulated *F*-value ($F_{6, 9, 0.05}$ = 3.37) which implies that eqn. (5) has a good prediction of the RON model and that the estimated factor effects are real at 95% confidence level.

Table **6** demonstrates the evaluated *t*-Student's distribution test and the corresponding *p*-values. The single-factor term represents a linear effect of the corresponding factor, while the two factors represent the interaction between the two factors. Additionally, the second order term represents a quadratic effect towards the response. The *p*-value serves as a tool to check the significance of each coefficient at a specified level of significance. The higher the *t*-value or the smaller the *p*-value the more significant is the corresponding coefficient. Generally, a *p*-value of less than < 0.05 is considered to be very significant and contributes largely towards the responses. As illustrated in Table **6**, the linear reaction temperature term (X_1), has the largest effect on RON at the 99.7% confidence level of significance as indicated by the lowest *p*-value of (<0.003) and the highest absolute *t*-value (5.18).

Next, the linear term of total pressure (X_2) could also be considered as a significant factor affecting the RON (*P*-value < 0.05) at the 95% confidence level followed by the effect of contact time (LHSV, hr^{-1}) (X_3) and the quadratic term (X_2^2) of pressure which appeared a statistical significant at 94% and 91%, respectively. According to *t*- and *p*- values sorted in Table **6**, the significance order of the independent variables on the maximum obtained RON is reaction temperature, operating pressure and space velocity, respectively. However, the other terms are not statistically significant.

Figure **6** represents the 3-D plot of RON model in an estimated response over the process conditions (reaction temperature and operating pressure) depicted at fixed space velocity. The figure reveals that RON has been enhanced of up to 110 as the temperature increased up to 530^oC at operating pressure in the range between 5-10 bar. This can be attributed to the fact that raising the reaction temperature favored the formation of aromatics and olefin hydrocarbons.

Table 5: ANOVA Results Table for *RON* Value

Sources	Sum of Squares	Degree of Freedom	Mean Squares	$F_{(calculated)}$ Value	$F_{(Tabulated)}$ (6,9,0.05)
S.S. Regression	264.362	9	29.373	5.147	>3.37
S.S. Error	34.2352	6	5.705		
S.S. Total	298.5972	15			

Table 6: Multiple Regression Results and Sorted Significance Effect of Regression Coefficient for RON Model

Parameter	Term	Coefficient	*t-value*	*p-value*
β_1	X_1	-2.9024	5.18284	0.002049
β_2	X_2	-4.1514	-2.58383	0.041555
β_3	X_3	1.8125	-2.33331	0.058376
β_{22}	X_2^2	0.0153	2.06595	0.084359
β_{12}	X_1X_2	0.0060	1.07012	0.325713
β_{11}	X_1^2	0.0031	0.93561	0.385583
β_{23}	X_2X_3	0.2629	0.93395	0.386374
β_{13}	X_1X_3	-0.0286	-0.15245	0.883828
β_{33}	X_3^2	0.7218	0.08786	0.932848
R^2	*0.885*			

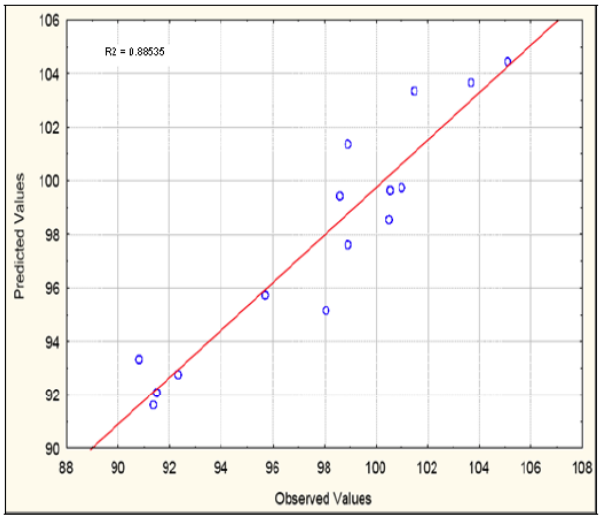

Figure 5: Comparison between predicted and observed RON values

However, these hydrocarbons have high octane numbers that tend to enhance the RON of reformate [24].

Aromatization Activity (Single-Response Optimization)

Investigations of the best variables of reaction temperature, operating pressure and space velocity in the Pt-Re-Sn catalyst were studied in order to decrease the aromatization activity. An empirical relationship represented as mathematical model between aromatization activity and the test variables in coded unit is given in eqn (6). Indeed, the empirical model developed in eqn (2) by applying multiple regression technique was fitted to the experimental results. Figure **7** compares the experimental yield of aromatization activity model with the predicted one obtained from Eq. (6) and the aromatization activity model fitted well with the experimental results.

$$Y_A = - 406.516+1.931x_1 -13.054\ x_2 + 22.364x_3 - 0.002 x_1^2 + 0.026_{X2}{}^2 +19.570$$

$$x_3^2 + 0.022X_1\ X_2 - 0.211x_1x_3 + 0.443x_2x_3 \qquad (6)$$

where Y_A is the predicted value for the aromatization activity.

A reasonable value of determination coefficient R^2=0.806 was obtained to estimate the regression coefficients which gives an indication of an acceptable agreement between the observed and predicted data. It is worth mentioning here, that the determination coefficient R^2 is fairly lower than the RON model. Thus,

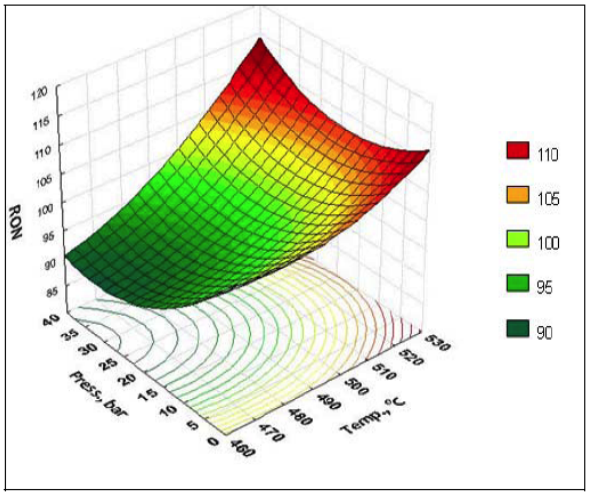

Figure 6: 3-D Response surface plot for the design of RON as a function of reaction temperature and operating pressure depicted at fixed space velocity.

Table 7: ANOVA Results Table for Aromatization Activity

Sources	Sum of Squares	Degree of Freedom	Mean Squares	F value	F (6,9,0.05)
S.S. Regression	1571.272	9	369.193	5.857	>3.37
S.S. Error	378.193	6	63.0321		
S.S. Total	1949.465	15			

Table 8: Multiple Regression Results and Sorted Significance Effect of Regression Coefficient for Aromatization Activity

Parameter	Term	Coefficient	*t*-value	*p*-value
β_1	$X1$	1.931	3.22196	0.018092
β_2	$X2$	-13.054	-2.58273	0.041617
β_3	$X3$	22.364	-2.05543	0.085596
β_{12}	X_1X_2	0.022	1.16690	0.287525
β_{22}	X_2^2	0.026	1.09437	0.315769
β_{33}	X_3^2	19.570	0.75000	0.481618
β_{23}	X_2X_3	0.443	0.47461	0.651845
β_{13}	X_1X_3	- 0.211	-0.33901	0.746154
β_{11}	X_1^2	- 0.002	-0.12947	0.901218
R^2	*0.885*			

the RON model exhibits a better fit than the aromatization activity model. The adequacy of the model was tested with analysis of variance as shown in Table **7**, where the computed *F*-value of 5.857 was higher than the tabulated *F*-value ($F_{6, 9, 0.05} = 3.37$).

Table **8** shows the multiple regression results and significance of each regression coefficient of the aromatization activity model. The terms of the model were arranged based on *t- and p-* values signifying the variable effects on the aromatization activity model. According to lowest *p-* values less than 0.5 and highest *t*-student test values (3.22 and 2.58, respectively), the linear terms of reaction temperature and operating pressure (X_1 and X_2, respectively) are the most influential parameters on the aromatization activity at confidence level of 98% and 95% of significance, respectively. However, the space velocity exhibited a small effect at 91% level. In addition, the influences of the other terms were statistically insignificant.

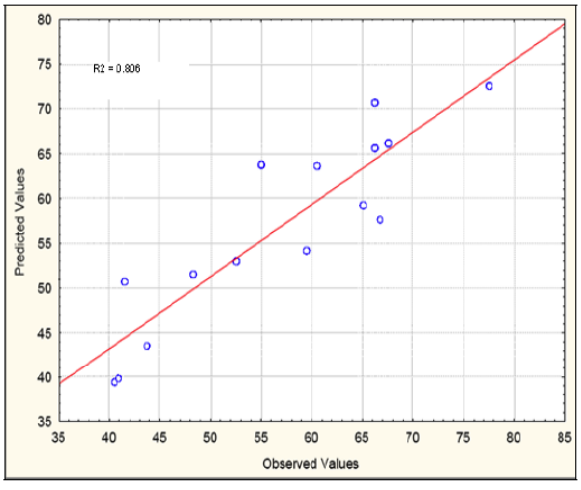

Figure 7: Comparison between predicted and observed values of aromatization activity.

Figure **8** shows the contour plot of the aromatization activity with the pressure and space velocity at a zero level of other variables (fixed reaction temperature). The figure shows clearly an inclined profile implying the interactions effect between both factors on the aromatization activity. It can be noticed that low pressure and high contact time (low space velocity) lead to enhance the aromatization activity due to high aromatization activity under these conditions. From (RSM) (statistic software), the optimum minimum point for the aromatization activity is 40.4% when pressure is 30 bar and space velocity is 1.8 hr^{-1}.

The *3-D* plot presented in Figure **9** shows the estimated aromatization activity over the reaction temperature and operating pressure at fixed space velocity. It is worth to mention that increasing pressure leads to suppress the formation of aromatics. It can be revealed form the Figure that low reaction temperature of 460°C with high operating pressure of 35 bar leads to a low aromatization activity of 20%. According to the reforming reactions mechanism which classified as Preferable and non-preferable reactions, this fact can attributed to the decrease of de/hydrogenation activity of the catalyst which responsible for the selectivity and stability in the reforming reactions.

As shown in the Figure **9**, decreasing the pressure leads to improve the aromatization activity by favoring dehydrogenation of naphthenes and dehydrocyclization of paraffins and thus suppress hydro-racing reactions. However, the higher selectivity of aromatization reactions at low hydrogen pressures indicates the possible importance of unsaturated intermediates and the stepwise aromatization pathway where alkenes transformed in further reactions, mainly to aromatics but other products are not excluded [25-26].

It can revealed that the reaction temperature progressively enhances the aromatization activity, by increasing the reaction temperature up to 520°C the aromatization activity was increased as the maximum predicted value at 80%. As the *RON* model show a large contribution of the linear term X_1 of the temperature variable However, the lower aromatization activity at low reaction temperature can be lead to a substational decrease in research octane number of reformats. This fact is in good agreement with the results reported earlier revealed that there is a strong correlation between aromatics content of reformats and RON. However, high octane numbers is achievable through extensive paraffin dehydrocyclization, Indeed, loss of *RON* can partially be compensated by the increase of the amount of i-paraffins in reformates.

Isomerization Activity Model (Single Response Optimization)

In this section, maximum response of isomerization activity was achieved using *RSM*. The coefficients of isomerization activity model as obtained from eqn (2) were estimated using multiple regression analysis in the RSM. Eq. (7) represents the response surface model of isomers selectivity (I_{somers})

$$I_{somers} = - 225.488+1.492x_1 + 16.483x_2 -204.528x_3 - 0.002x_1^2 -0.043x_2^2 -16.555$$

$$x_3^2 -0.028x_1x_2 + 0.544x_1x_3 -0.048x_2x_3 \quad (7)$$

where, I_{somers} is the predicted percentage of saturated hydrocarbons compounds.

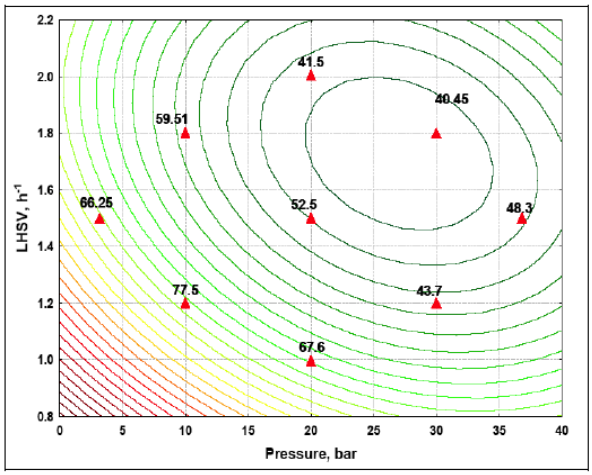

Figure 8: 2-D contour surface plot of aromatization activity as a function of pressure and space velocity depicted at fixed temperature

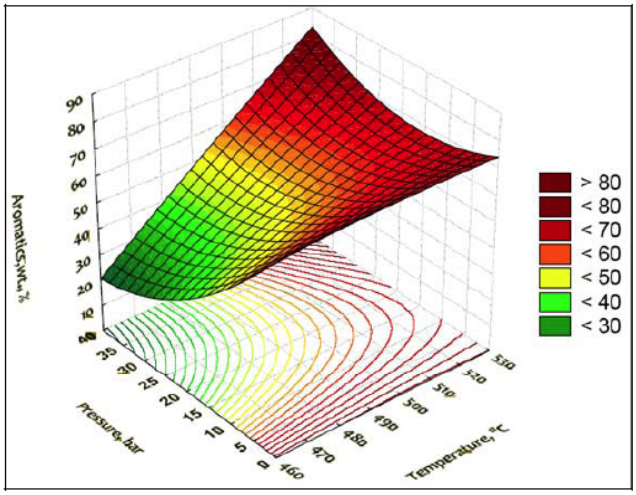

Figure 9: 3-D Response surface plot for the design of aromatization activity as a function of reaction temperature and operating pressure depicted at fixed space velocity

As shown in Figure **10**, the regression coefficients of eqn (7) indicated an acceptable fit between the observed and the predicted data. The determinant of coefficient R^2 equals to 0.839 indicated that this model is sufficient to explain most of the variation in the response. The adequacy of the isomers selectivity model was checked with ANOVA. From Table **9** of ANOVA analysis results, the calculated Fisher test (F) value for isomers selectivity model is 3.50 which is higher than the tabulated one ($F_{6,9,0.05}$=3.37), showing that this model is significant at the selected confidence level (95%).

As shown in Table **10**, the multiple regression results are arranged based on the significance of regression coefficients for the isomers selectivity

Table 9: ANOVA Results Table for Isomerization Activity

Sources	Sum of Squares	Degree of Freedom	Mean Squares	F value	F (6,9,0.05)
S.S. Regression	1983.681	9	220.409	3.50	>3.37
S.S. Error	380.630	6	63.0321		
S.S. Total	2364.311	15			

Table 10: Multiple Regression Results and Sorted Significance Effect of Regression Coefficient for Isomerization Activity

Parameter	Term	Coefficient	*t*-Value	*p*-Value
β_1	$X1$	1.492	-3.58172	0.011619
β_2	$X2$	16.483	2.80862	0.030812
β_3	$X3$	-204.528	2.00038	0.092377
β_{22}	X_2^2	-0.043	-1.74327	0.131913
β_{12}	X_1X_2	-0.028	-1.51723	0.180001
β_{13}	X_1X_3	0.544	0.86914	0.418174
β_{33}	X_3^2	-16.555	-0.60437	0.567730
β_{11}	X_1^2	- 0.002	-0.20671	0.843076
β_{23}	X_2X_3	-0.048	-0.05060	0.961284
R^2	*0.839*			

model. From the data shown in Table **10**, the significant variables are sorted according to their *t*-and *p*-values, the lower *p*- value with a higher *t*- value as *t* and *p* values indicate the highly significant corresponding coefficients. Based on this fact, the linear term of reaction temperature (X_1) in this model statistically has the highest influence on the isomers selectivity at 98% confidence level of significance followed by the linear term of operating pressure (X_2). However, the linear term of space velocity (X_3) also showed a slight effect at 92 % confidence level.

Figure **11** presents the 3-D graphical surface plot of isomerization activity for temperature and pressure. From the figure, it can be noticed that the high reaction temperature leads to minimize isomerization activity to 18 %. This is attributed to the fact that straight chain alkanes are favorably converted into cyclic hydrocarbons at high temperature which are thermodynamically privileged. The so called intermediate hydrocarbons (Olefins, iso-olefins and i-paraffins) produced from the dehydrogenation reactions on the metal site (alkenes) and from isomerization reactions on the acid sites (iso-alkenes) followed by hydrogenated reactions to (iso-alkanes) are unstable and easily transformed to aromatics hydrocarbons (C_6-C_8) and light ends (C_1-C_4) due to successive reactions (aromatization and cracking). This phenomenon confirms the fact that high reforming temperature is not selective to enhance isomerization activity.

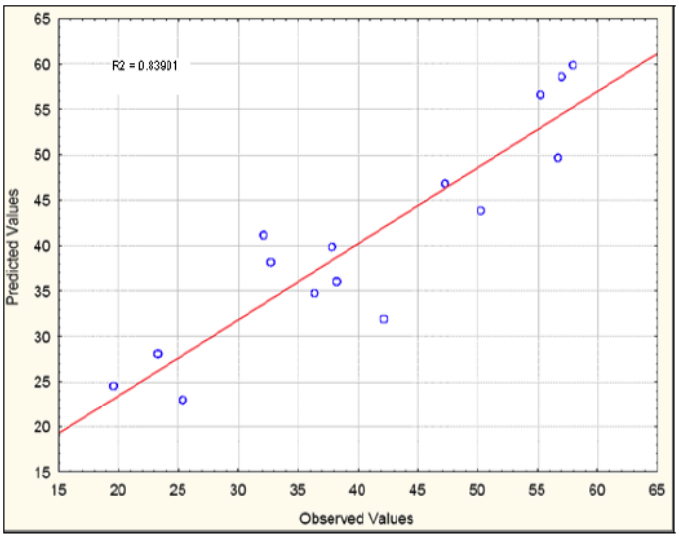

Figure 10: Comparison between predicted and observed values for isomerization activity

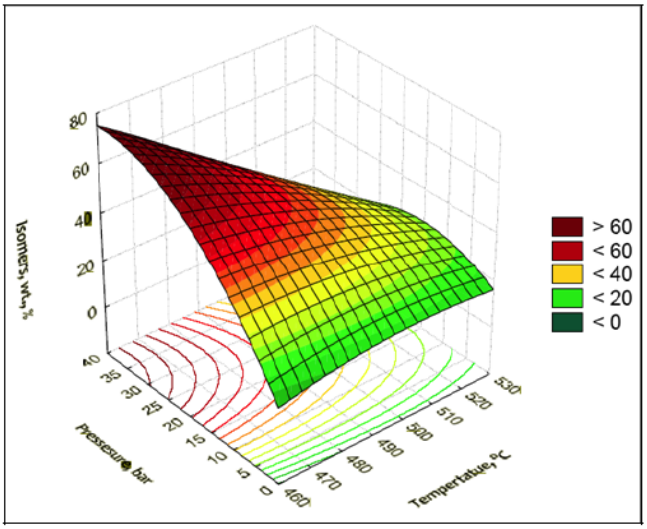

Figure 11: 3-D Response surface plot for the design, isomerization activity as function of reaction temperature and operating pressure

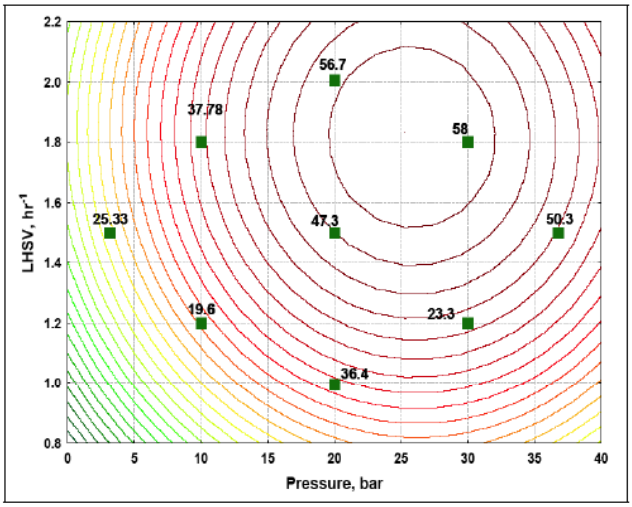

Figure 12: 2-D contour surface plot of isomerization activity as a function of pressure and space velocity depicted at fixed temperature

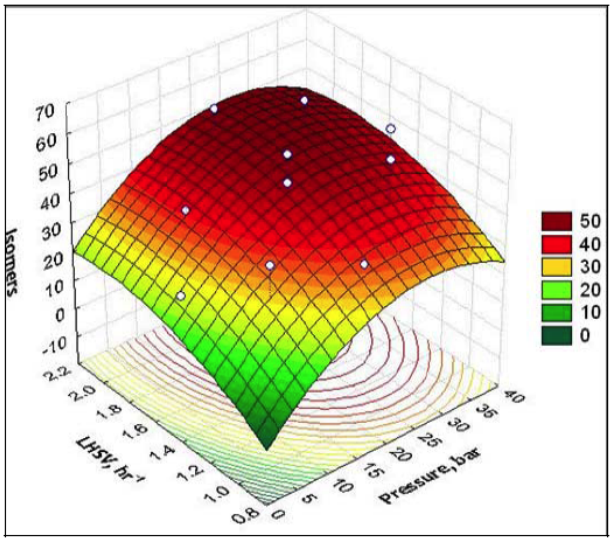

Figure 13: 3-D Response surface plot for the design, isomerization activity as function of reaction pressure and space velocity.

Figure **12** which present the 2D contour plot of isomerization activity for operating pressure and space velocity at fixed temperature. The Figure revealed a ring of complete round profile implying the interaction effect between both factors on the response. The maximum predicted selectivity is indicated by the surface confined in the smallest circle in the contour diagram. It is clearly the isomerization activity reached its maximum at a combination of coded level 1.6-2.2hr $^{-}$1 of LHSV and 20-30 of operating pressure. The model predicted optimum point for maximum isomerization activity of 58% when pressure is 30 bar and space velocity is 1.8 h.

Moreover, it can reveal from Figure **13** of 3D plot depicted at fixed temperature that decreasing the pressure from 15 to 5 bars resulted in a decrease in isomerization activity to less than 20 %. As shown in

Table 11: Independent Optimal Values of Aromatization Activity from Single Response Optimization

Independent Variables (*X*)	Location of Optimum	Aromatization Activity (%)
Reaction Temperature (*X*1) (^{o}C)	535.4	60.0
Operating pressure (*X*2) (bar)	8.3	
Space velocity (*X*3) (hr^{-}1)	2.1	

Table 12: Independent Optimal Values of Isomerization Activity from Single Response Optimization

Independent Variables (*X*)	Location of Optimum	Isomerization Activity (%)
Reaction Temperature (X_1) (^oC)	537.1	41.5
Operating pressure (X_2) (bar)	12.4	
Space velocity (X_3) (hr^-1)	2.5	

Table 13: Independent Optimal Values of RON from Single Response Optimization

Independent Variables (*X*)	Location of Optimum	Maximum RON
Reaction Temperature (*X*1) (^oC)	449.9	89
Operating pressure (*X*2) (bar)	32.5	
Space velocity (*X*3) (hr^-1)	1.7	

Table 14: Comparison between Predicted and Observed Responses at Optimum Condition (Reaction Temperature = 449 ^oC, Operating Pressure = 32 bar and LHSV = 1.7 h^{-1}) Obtained from RSM

Responses	Predicted Value	Observed Value	Error (%)
RON value	89	90.0	1.93

Figure **12**, the minimum point for isomerization activity is 19.6 % when pressure is 10 bar and space velocity is 1.2 hr^{-1}. However, low pressure favors the coke formation and aromatization activities. The enhancement of isomerization activity of the catalyst coupled with low aromatization activity towards the intermediate products (Olefins) was observed under high operating pressure and high space velocity.

It is worthy to mention here that the changes in LHSV can have a significant effect on the reformate quality (RON) as well as its yield. However, according to thermodynamic point of view, reactions such as aromatization and isomerization, in general, are not as much affected by varying the space velocity, because these desirable reactions are occurred very fast and can reach equilibrium rapidly even at higher space velocities.

Multi-Variables Single Response Optimization

The optimization of the multi-variables single-response was determined by using Nelder–Mead Simplex technique. Tables **11-13** tabulate the independent optimal values of the single responses optimization of aromatization activity, isomerization activity, and RON, respectively, together with the corresponding optimal values of their independent variables (X_1, X_2 and X_3). As shown in Table **11**, the aromatization activity reached a maximum value of 60% at the corresponding optimal factors of reaction temperature, operating pressure and space velocity being 535.4 ^oC, 8.3 bar, and 2.1hr^{-1}, respectively. The results of the single-response optimization were close to the results obtained by Ali *et al.* [8] and Moljord *et al* [10] in which a high aromatic selectivity was attained at higher reaction temperature and low operating pressure.

In addition, the maximum isomerization activity is achieved at 41.5 % with respect to reaction temperature, operating pressure and space velocity of 537^oC, 12.4 bar, and 2.5 hr^{-1}%, respectively, as presented in Table **12**. It can be noticed that increasing pressure from 8 to 12 bars as well as increasing the space velocity led to enhanced i-paraffins and reduced aromatics content of the reformate [8,9].

Optimization of RON using Response Surface Methodology

In this work, only RON was optimized. However, the value for the RON is the product of the concentration of aromatics and i-paraffins hydrocarbons. As shown in Table **13**, the response surface analysis indicates that the predicted maximum RON yield was 89.2 at reaction temperature = 449.9 ^oC, operating pressure = 32.5 bar and LHSV = 1.7 h^{-1}. Additional experiments were

performed to validate the optimization results obtained by the response surface methodology analysis. It can be noticed that the predicted value of RON was reasonable with respect to the corresponding operating conditions presented in Table **13**.

The comparison between the experimental and predicted data for RON at optimum conditions is shown in Table **14**. The experimental value obtained was 93.0; the difference between the predicted and observed results is 4.3%. The errors can be considered small as the observed values are within the 95% confidence intervals.

CONCLUSIONS

The influences of reaction temperature, operating pressure and LHSV on catalytic naphtha reforming process were studied over Pt-Re-Sn/Al_2O_3 catalyst. Central composite design (CCD) coupled with response surface methodology (RSM) were employed. The design guided to three surface responses on the dependence of RON yield, aromatization activity, and isomerization activity on reaction temperature (480-510 ^oC), operating pressure (10-30 bar) and LHSV (1.2-1.8 h^{-1}). The equation models were tested with analysis of variance with 95% degree confidence. The results of the analysis concluded that the equation models fitted well with the experimental results for naphtha reforming process to produce optimum RON of reformates. Numerical results indicated that the maximum RON was 89 at optimum reaction temperature of 449^oC, operating pressure of 32 bar and LHSV of 1.7 h^{-1-}. Additional experiments were performed at the defined optimum conditions for verification of aromatization activity and isomerization activity.

ACKNOWLEDGEMENTS

The authors would like to express their sincere gratitude to Professor J.L. Margitfalvi and Dr. S. G"obölös of Institute of Chemistry, Chemical Research Center, Hungarian Academy of Sciences, for the consultant support. The authors would also like to thank Miss I. Borbáth, M. for her assistance in the preparation of catalyst.

REFERENCES

[1] Arribas MA, Márquez F, Martı, amp, ´nez A. Activity, Selectivity, and Sulfur Resistance of Pt/WOx–ZrO2 and Pt/Beta Catalysts for the Simultaneous Hydroisomerization of n-Heptane and Hydrogenation of Benzene. Journal of Catalysis 2000; 190(2): 309-19.

[2] Grau JM, Vera CR, Parera JM. Preventing self-poisoning in [Pt/Al2O3 + SO42−-ZrO2] mixed catalysts for isomerization-cracking of heavy alkanes by prereduction of the acid function. Applied Catalysis A General 2002; 227(1–2): 217-30.

[3] Elfghi F, Amin NAS. Applying response surface methodology to assess the combined effect of process variables on the composition and octane number of reformat in the process of reducing aromatization activity in catalytic naphtha reforming. Reac Kinet Mech Cat 2014 2014/02/01; 111(1): 89-106.

[4] Stikkers DE. Octane and the environment. Science of The Total Environment 2002; 299(1–3): 37-56.

[5] Seddon D. Reformulated gasoline, opportunities for new catalyst technology Catal Today 1992; 15(1): 1-21.

[6] Rossini S. The impact of catalytic materials on fuel reformulation Catal Today 2003; 77(4): 467-84.

[7] Benadda A, Katrib A, Barama A. Hydroisomerization of n-heptane and dehydration of 2-propanol on MoO2(Hx)ac. catalysts. Applied Catalysis A General 2003; 251(1): 93-105.

[8] Ali SA, Mohammed AS, and Mohammed AA. Parametric study of catalytic reforming process. React Kinet Catal Lett 2005 2005/12/01; 87(1): 199-206.

[9] Fürcht Á, Tungler A, Szabó S. n-Octane Reforming: Conversion And Selectivity Dependence On Space Velocity. React Kinet Catal Lett 2001 2001/03/01; 72(2): 269-75.

[10] Moljord K, Hellenes HG, Hoff A, Tanem I, Grande K, Holmen A. Effect of reaction pressure on octane number and reformate and hydrogen yields in catalytic reforming. Ind Eng Chem Res 1996; 35: 99-105.

[11] Larentis AL, de Resende NS, Salim VMM, Pinto JC. Modeling and optimization of the combined carbon dioxide reforming and partial oxidation of natural gas. Appl Catal A: Gen 2001; 215: 211-224.

[12] Rezzoug SA, Capart R. Assessment of wood liquefaction in acidified ethylene glycol using experimental design methodology. Energy Conver Mgmt 2003; 44: 781-792

[13] Nele M, Vidal A, Bhering DL, Pinto JC, Salim VMM. Preparation of high loading silica supported nickel catalyst: simultaneous analysis of the precipitation and aging steps. Appl Catal A Gen 1999; 178: 177- 189.

[14] Yoon WL, Park JS, Jung H, Lee HT, Lee DK. Optimization of pyrolytic coprocessing of waste plastics and waste motor oil into fuel oils using statistical pentagonal experimental design Fuel 1999; 78: 809-813.

[15] Bishara A, Stanislaus A, Hussain SS. Effect of feed composition and operating conditions on catalyst deactivation and on product yield and quality during naphtha catalytic reforming Appl Catal 1984; 13: 113-125.

[16] A.Furcht, A.Tungler, S.Szabo, Z.Schay, L.Vida, I.Gresits, n-Octane reforming over modified catalysts: II. The role of Au Ir and Pd Appl Catal A 2002; 231: 151-157

[17] Haaland PD. Experimental Design in Biotechnology. New York Marcel Dekker Inc 1989.

[18] Montgomery DC. Design and Analysis of Experiments. New York John Wiley & Sons 2001.

[19] Clarke GM, Kempson RE. Introduction to the Design and Analysis of Experiments. London: Arnold; 1997.

[20] Cornell J.A. How to Apply Response Surface Methodology. The Basic References in Quality Control: Statistical Techniques, American Society for Quality Control Wisconsin 1990. Vol. 8 p. 1-82

[21] Box GEP, Hunter WG, Hunter JS. Statistics for Experimenters: An Introduction to Design, Data Analysis, and Model Building. New York: John Wiley & Sons; 1978

[22] Brown SR, Melamed LE. Experimental Design and Analysis. Quantitative Applications in the Social Sciences. California: stage publications 74; 1990.

[23] Montgomery DC, Runger GC, Hubele NF. Design of Engineering Experiments. in: Engineering Statistics. 3rd ed Wiley 2003, p. 317-388.

[24] Paal Z, Gyory A, Uszkurat I, Olivier S, Guerin M, Kappenstein C. Pt/Al2O3 catalysts and Pt–Sn/Al2O3 catalysts prepared by two different methods: hydrogen pressure effects in the reactions of n-Hexane. J Catal 1997; 168: 164-175.

[25] Paal Z, Xu X. L, PaalLukacs J , Vogel W, Muhler M, Schlogl R. Platinum-Black Catalysts sintered at Different temperatures: Surface Analysis and Activity in Reactions of n-Hexane, J Catal 1995; 152- 252

[26] Paal Z, Tetenyi P, The Mechanism Of Aromatization On Platinum Black Catalyst; Dehydrocyclyzation of Hexadienes and Hexatrienes, J Catal 1973; 30-350.

Received on 30-09-2014 Accepted on 03-11-2014 Published on March-2015

http://dx.doi.org/10.15379/2408-9834.2015.02.01.1